

---

# JOURNAL OF THE AMERICAN CHEMICAL SOCIETY

---

## Minimal Lipidation Stabilizes Protein-Like Molecular Architecture

Ying-Ching Yu,<sup>†,‡</sup> Matthew Tirrell,<sup>‡</sup> and Gregg B. Fields<sup>\*,†,§</sup>

Contribution from the Departments of Laboratory Medicine & Pathology and Chemical Engineering & Materials Science, University of Minnesota, 420 Delaware Street S.E., Minneapolis, Minnesota 55455, and Department of Chemistry & Biochemistry, Florida Atlantic University, 777 Glades Road, Boca Raton, Florida 33431-0991

Received May 12, 1998

**Abstract:** Peptide-amphiphiles with collagen-model head groups and dialkyl chain tails have been shown previously to self-assemble into highly ordered polyPro II-like triple-helical structures when dissolved in aqueous subphases. In the present study, we have examined peptide-amphiphiles containing monoalkyl chain tails for similar self-assembly behaviors. The structure of a collagen-model peptide has been characterized with and without an *N*-terminal hexanoic acid (C<sub>6</sub>) modification. Evidence for a self-assembly process of both the peptide and peptide-amphiphile has been obtained from (a) circular dichroism spectra and melting curves characteristic of triple-helices, (b) one-dimensional NMR spectra indicative of stable triple-helical structure at low temperatures and melted triple helices at high temperatures, and (c) pulsed-field gradient NMR experiments demonstrating different self-diffusion coefficients between proposed triple-helical and non-triple-helical species. The peptide-amphiphile appeared to form monomeric triple helices. The thermal stability of the collagen-like structure in the peptide-amphiphile was found to increase as the monoalkyl tail chain length is increased over a range of C<sub>6</sub> to C<sub>16</sub>. The assembly process driven by the hydrophobic tail, albeit monoalkyl or dialkyl, may provide a general method for creating well-defined protein molecular architecture. Peptide-amphiphile structures possessing these alkyl moieties have the potential to be used for biomaterial surface modification to improve biocompatibility or, by mimicing fusion of viral envelopes with cellular membranes, as drug delivery vehicles.

### Introduction

The creation of protein-like molecular architectures relies on an organized assembly of individual peptide strands. Two approaches for inducing assembly are (a) the incorporation of templates to covalently link individual strands and (b) the application of moieties that allow for noncovalent self-assembly of individual strands.<sup>1</sup> One structural element that has been induced and stabilized by both approaches is the collagen triple

helix. The triple helix consists of three polypeptide chains, each in an extended, left-handed polyPro II-like helix, which are staggered by one residue and then supercoiled along a common axis in a right-handed manner.<sup>2</sup> Geometric constraints of the triple-helical structure require that every third amino acid is Gly, resulting in a Gly-X-Y repeating sequence. Substantial stabilization of the triple-helical structure can be achieved with the introduction of a dilysine or diglutamate template at the C- or

<sup>†</sup> Department of Laboratory Medicine & Pathology, University of Minnesota.

<sup>‡</sup> Department of Chemical Engineering & Materials Science, University of Minnesota.

<sup>§</sup> Florida Atlantic University.

(1) See recent review: Mayo, K. H.; Fields, G. B. In *Protein Structural Biology in Bio-Medical Research*; Allewell, N. M., Woodward, C., Eds.; JAI Press Inc.: Greenwich, CT, 1997; pp 567–612.

(2) (a) Brodsky, B.; Shah, N. K. *FASEB J.* **1995**, *9*, 1537–1546. (b) Brodsky, B.; Ramshaw, J. A. M. *Matrix Biol.* **1997**, *15*, 545–554.

N-terminal regions of the three peptide chains<sup>3-7</sup> or by using a Kemp triacid template linked to the N-terminus of three peptide chains.<sup>8</sup> Conversely, a noncovalent, self-assembly approach to building a collagen-like structural motif which uses the alignment of amphiphilic compounds at the lipid-solvent interface to facilitate peptide alignment and structure initiation and propagation has been reported.<sup>9,10</sup>

Ideally, one would like to create the simplest system possible by which synthetic linear peptide chains self-assemble into desirable secondary and tertiary structures. Since collagen-like structures are well defined and reasonably easy to construct, it is an ideal structural element for characterizing self-assembly approaches. The triple helix is found in a variety of proteins in addition to collagen, such as macrophage scavenger receptors types I and II<sup>11</sup> and bacteria-binding receptor MARCO,<sup>12</sup> complement component C1q,<sup>13</sup> pulmonary surfactant apoprotein,<sup>14</sup> acetylcholinesterase,<sup>15</sup> and mannose binding protein.<sup>16</sup> The potential activities mediated by triple helices are quite varied. For our purposes, we have chosen to study the self-assembly behavior of a type IV collagen-derived cell adhesion site. The  $\alpha 1(\text{IV})1263-1277$  collagen sequence Gly-Val-Lys-Gly-Asp-Lys-Gly-Asn-Pro-Gly-Trp-Pro-Gly-Ala-Pro ([IV-H1]) is known to promote melanoma cell adhesion and spreading.<sup>3,17,18</sup> Triple-helical conformation greatly enhances the

biological activity of [IV-H1].<sup>3,10,19</sup> The [IV-H1] sequence alone, as well as many other biologically active collagen sequences, does not form a triple helix in solution.<sup>18,20</sup> There are several strategies for creating biologically active triple-helical collagen models.<sup>2,20</sup> In previous studies, we have described the synthesis of novel dialkyl peptide-amphiphiles containing the [IV-H1] sequence.<sup>9,21</sup> The resulting peptide-amphiphiles were found to self-assemble to form stable triple helices under physiological conditions.<sup>9</sup> Triple-helical structure of the peptide-amphiphiles was confirmed by circular dichroism (CD) spectroscopy and two-dimensional NMR spectroscopy of the Pro and Hyp side chains within and/or surrounding the [IV-H1] site.<sup>9</sup> The thermal stability of the triple helix was significantly enhanced in the peptide-amphiphile compared with that of the peptide alone. The hydrophobic interactions of the lipid tails were found to play an important role in the formation of stable protein motifs.<sup>9</sup>

In the present study, we have examined monoalkyl chain tails for their ability to stabilize triple-helical structure. It is important to better understand the general effect of lipidation on protein-like structure beyond that of dialkyl tails, as lipids may then be selected for specific applications. There are several reasons as to why monoalkyl peptide-amphiphiles are more desirable than dialkyl peptide-amphiphiles. First, synthesis of monoalkyl peptide-amphiphiles is much simpler than that of dialkyl peptide-amphiphiles. Second, dialkyl peptide-amphiphiles readily aggregate to form higher order structures such as micelles and vesicles, which make NMR structural characterization difficult due to line broadening. A single-chain amphiphile is less likely to form as extensive higher order structures, as the size of the lipid tail is small and the hydrophobic interaction is weaker than that of the longer dialkyl peptide-amphiphiles. The overall result is potentially sharper NMR spectral lines which will help to distinguish small differences in chemical shifts. In the present study, we have used CD and NMR spectroscopies to (1) provide evidence that monoalkyl peptide-amphiphiles are in triple-helical conformation, (2) investigate the [IV-H1] region to see if a biologically active sequence within a peptide-amphiphile is in triple-helical conformation, and (3) investigate the effect of monoalkyl lipidation on triple-helical thermal stability. Triple-helical structure has been characterized by comparison of our CD and NMR spectroscopic data to prior studies of collagen and collagen-model peptides in which triple helicity has been confirmed by a combination of X-ray crystallographic and CD and NMR spectroscopic analyses.

## Experimental Section

**Synthesis of Peptides and Peptide-Amphiphiles.** All standard peptide synthesis chemicals and solvents were analytical reagent grade or better and were purchased from Applied Biosystems, Inc. (Foster City, CA) or Fisher Scientific (Pittsburgh, PA). Fmoc-4-(2',4'-dimethoxyphenylaminomethyl)phenoxy resin (substitution level = 0.46 mmol/g) was purchased from Novabiochem (La Jolla, CA). All Fmoc-amino acid derivatives were from Novabiochem and are of L-configuration. 1-Hydroxybenzotriazole (HOBt) was purchased from Novabiochem, 2-(1H-benzotriazole-1-yl)-1,1,3,3-tetramethyluronium hexafluorophosphate (HBTU) from Richelieu Biotechnologies (St. Hyacinthe, Quebec), and *N,N*-diisopropylethylamine (DIEA) from Fisher Scientific. The monoalkyl chains used in this study, hexanoic acid [ $\text{CH}_3(\text{CH}_2)_4\text{CO}_2\text{H}$ , designated C<sub>6</sub>], octanoic acid [ $\text{CH}_3(\text{CH}_2)_6\text{CO}_2\text{H}$ , designated C<sub>8</sub>], decanoic acid [ $\text{CH}_3(\text{CH}_2)_8\text{CO}_2\text{H}$ , designated C<sub>10</sub>],

(3) Fields, C. G.; Mickelson, D. J.; Drake, S. L.; McCarthy, J. B.; Fields, G. B. *J. Biol. Chem.* **1993**, *268*, 14153-14160.

(4) (a) Fields, C. G.; Lovdahl, C. M.; Miles, A. J.; Matthias Hagen, V. L.; Fields, G. B. *Biopolymers* **1993**, *33*, 1695-1707. (b) Grab, B.; Miles, A. J.; Furcht, L. T.; Fields, G. B. *J. Biol. Chem.* **1996**, *271*, 12234-12240.

(5) (a) Roth, W.; Heppenheimer, K.; Heidemann, E. R. *Makromol. Chem.* **1979**, *180*, 905-917. (b) Roth, W.; Heidemann, E. *Biopolymers* **1980**, *19*, 1909-1917. (c) Thakur, S.; Vadolas, D.; Germann, H.-P.; Heidemann, E. *Biopolymers* **1986**, *25*, 1081-1086. (d) Germann, H.-P.; Heidemann, E. *Biopolymers* **1988**, *27*, 157-163.

(6) (a) Fields, C. G.; Grab, B.; Lauer, J. L.; Fields, G. B. *Anal. Biochem.* **1995**, *231*, 57-64. (b) Fields, C. G.; Grab, B.; Lauer, J. L.; Miles, A. J.; Yu, Y.-C.; Fields, G. B. *Letts. Pept. Sci.* **1996**, *3*, 3-16.

(7) (a) Tanaka, T.; Wada, Y.; Nakamura, H.; Doi, T.; Imanishi, T.; Kodama, T. *FEBS Lett.* **1993**, *334*, 272-276. (b) Tanaka, T.; Nishikawa, A.; Tanaka, Y.; Nakamura, H.; Kodama, T.; Imanishi, T.; Doi, T. *Protein Eng.* **1996**, *9*, 307-313. (c) Hojo, H.; Akamatsu, Y.; Yamauchi, K.; Kinoshita, M.; Miki, S.; Nakamura, Y. *Tetrahedron* **1997**, *53*, 14263-14274. (d) Tanaka, Y.; Suzuki, K.; Tanaka, T. *J. Pept. Res.* **1998**, *51*, 413-419.

(8) (a) Goodman, M.; Feng, Y.; Melacini, G.; Taulane, J. P. *J. Am. Chem. Soc.* **1996**, *118*, 5156-5157. (b) Goodman, M.; Melacini, G.; Feng, Y. *J. Am. Chem. Soc.* **1996**, *118*, 10928-10929. (c) Feng, Y.; Melacini, G.; Goodman, M. *Biochemistry* **1997**, *36*, 8716-8724.

(9) Yu, Y.-C.; Berndt, P.; Tirrell, M.; Fields, G. B. *J. Am. Chem. Soc.* **1996**, *118*, 12515-12520.

(10) Yu, Y.-C.; Pakalns, T.; Dori, Y.; McCarthy, J. B.; Tirrell, M.; Fields, G. B. *Methods Enzymol.* **1997**, *289*, 571-587.

(11) (a) Kodama, T.; Freeman, M.; Rohrer, L.; Zabrecky, J.; Matsudaira, P.; Krieger, M. *Nature* **1990**, *343*, 531-535. (b) Rohrer, L.; Freeman, M.; Kodama, T.; Penman, M.; Krieger, M. *Nature* **1990**, *343*, 570-572. (c) Ashkenas, J.; Penman, M.; Vasile, E.; Acton, S.; Freeman, M.; Krieger, M. *J. Lipid Res.* **1993**, *34*, 983-1000.

(12) Elomaa, O.; Kangas, M.; Sahlberg, C.; Tuukkanen, J.; Sormunen, R.; Liakka, A.; Thesleff, I.; Kraal, G.; Tryggvason, K. *Cell* **1995**, *80*, 603-609.

(13) Brodsky-Doyle, B.; Leonard, K. R.; Reid, K. B. *Biochem. J.* **1976**, *159*, 279-286.

(14) Benson, B.; Hawgood, S.; Schilling, J.; Clements, J.; Damm, D.; Cordell, B.; White, R. T. *Proc. Natl. Acad. Sci. U.S.A.* **1985**, *82*, 6379-6383.

(15) Schumacher, M.; Camp, S.; Maulet, Y.; Newton, M.; MacPhee-Quigley, K.; Taylor, S. S.; Friedmann, T.; Taylor, P. *Nature* **1986**, *319*, 407-409.

(16) (a) Drickamer, K.; Dordal, M. S.; Reynolds, L. *J. Biol. Chem.* **1986**, *261*, 6878-6887. (b) Oka, S.; Itoh, N.; Kawasaki, T.; Yamashina, I. *J. Biochemistry* **1987**, *101*, 135-144.

(17) Chelberg, M. K.; McCarthy, J. B.; Skubitz, A. P. N.; Furcht, L. T.; Tsilibary, E. C. *J. Cell Biol.* **1990**, *111*, 261-270.

(18) Mayo, K. H.; Parra-Diaz, D.; McCarthy, J. B.; Chelberg, M. *Biochemistry* **1991**, *30*, 8251-8267.

(19) Fields, G. B.; Lauer, J. L.; Dori, Y.; Fornis, P.; Yu, Y.-C.; Tirrell, M. *Biopolymers* **1998**, *47*, 143-151.

(20) See recent review: Fields, G. B. *Connect. Tissue Res.* **1995**, *31*, 235-243.

(21) Berndt, P.; Fields, G. B.; Tirrell, M. *J. Am. Chem. Soc.* **1995**, *117*, 9515-9522.

dodecanoic acid [ $\text{CH}_3(\text{CH}_2)_{10}\text{CO}_2\text{H}$ , designated  $\text{C}_{12}$ ], tetradecanoic acid [ $\text{CH}_3(\text{CH}_2)_{12}\text{CO}_2\text{H}$ , designated  $\text{C}_{14}$ ], and palmitic acid [ $\text{CH}_3(\text{CH}_2)_{14}\text{CO}_2\text{H}$ , designated  $\text{C}_{16}$ ], were purchased from Aldrich.

Peptide-resin assembly was performed by Fmoc solid-phase methodology on an ABI 431A peptide synthesizer.<sup>22,23</sup> All peptides and peptide-amphiphiles were synthesized as C-terminal amides to prevent diketopiperazine formation.<sup>24</sup> Peptide-resins were characterized by Edman degradation sequence analysis as described previously for "embedded" (noncovalent) sequencing.<sup>23</sup> Peptide-resins were then either (a) cleaved or (b) lipidated<sup>9</sup> with the appropriate  $\text{C}_n$  tail and then cleaved. Cleavage and side-chain deprotection of peptide-resins and peptide-amphiphile-resins proceeded for 2 h using ethanedithiol–thioanisole–phenol– $\text{H}_2\text{O}$ –TFA (2.5:5.5:5:82.5) as described.<sup>25</sup> Peptide-amphiphile cleavage solutions were extracted with methyl *tert*-butyl ether prior to purification.

**Peptide Purification and Analysis.** Preparative RP-HPLC purification was performed on a Rainin AutoPrep system. Peptides were purified with a Vydac 218TP152022  $\text{C}_{18}$  column (15–20- $\mu\text{m}$  particle size, 300- $\text{\AA}$  pore size, 250  $\times$  25 mm) at a flow rate of 5.0 mL/min. The elution gradient was either 0–60% B or 0–100% B in 60 min, where A was 0.1% TFA in  $\text{H}_2\text{O}$  and B was 0.1% TFA in acetonitrile. Detection was at 280 nm. Peptide-amphiphile purification was achieved using a Vydac 214TP152022  $\text{C}_4$  column (15–20- $\mu\text{m}$  particle size, 300- $\text{\AA}$  pore size, 250  $\times$  22 mm) at a flow rate of 5.0 mL/min. The elution gradient was 30–100% B in 70 min, where A was 0.05% TFA in  $\text{H}_2\text{O}$  and B was 0.05% TFA in 2-propanol. Detection was at 280 nm. Analytical RP-HPLC was performed on a Hewlett-Packard 1090 liquid chromatograph equipped with a Hypersil  $\text{C}_{18}$  column (5- $\mu\text{m}$  particle size, 120- $\text{\AA}$  pore size, 200  $\times$  2.1 mm) at a flow rate of 0.3 mL/min. The elution gradient was 0–60% B in 45 min, where A and B were the same as for peptide purification. Diode array detection was at 220, 254, and 280 nm.

Edman degradation sequence analysis was performed on an Applied Biosystems 477A Protein Sequencer/120A Analyzer. MALDI-TOF-MS was performed on a Hewlett-Packard G2025A LD-TOF mass spectrometer using a sinapinic acid matrix.<sup>9,21</sup> The following  $[\text{M} + \text{H}]^+$  values for peptides and peptide-amphiphiles were obtained: [IV-H1]-(Gly-Pro-Hyp)<sub>4</sub>, 2502.6 Da (theoretical 2502.7 Da); (Gly-Pro-Hyp)<sub>4</sub>-[IV-H1]-(Gly-Pro-Hyp)<sub>4</sub>, 3574.2 Da (theoretical 3574.9 Da);  $\text{C}_6$ -(Gly-Pro-Hyp)<sub>4</sub>-[IV-H1]-(Gly-Pro-Hyp)<sub>4</sub>, 3682.7 Da (theoretical 3673.1 Da);  $\text{C}_8$ -(Gly-Pro-Hyp)<sub>4</sub>-[IV-H1]-(Gly-Pro-Hyp)<sub>4</sub>, 3707.9 Da (theoretical 3701.1 Da);  $\text{C}_{10}$ -(Gly-Pro-Hyp)<sub>4</sub>-[IV-H1]-(Gly-Pro-Hyp)<sub>4</sub>, 3733.8 Da (theoretical 3729.2 Da);  $\text{C}_{12}$ -(Gly-Pro-Hyp)<sub>4</sub>-[IV-H1]-(Gly-Pro-Hyp)<sub>4</sub>, 3761.1 Da (theoretical 3757.2 Da);  $\text{C}_{14}$ -(Gly-Pro-Hyp)<sub>4</sub>-[IV-H1]-(Gly-Pro-Hyp)<sub>4</sub>, 3786.2 Da (theoretical 3785.3 Da);  $\text{C}_{16}$ -(Gly-Pro-Hyp)<sub>4</sub>-[IV-H1]-(Gly-Pro-Hyp)<sub>4</sub>, 3815.8 Da (theoretical 3813.3 Da).

**Circular Dichroism Spectroscopy.** Spectra were recorded on a JASCO J-710 spectropolarimeter using a thermostated 0.1-mm path-length thermally jacketed quartz cell. Temperature was controlled using a NESLAB water bath. CD spectra were obtained over a wavelength range  $\lambda = 190$ –250 nm. Thermal transition curves were obtained by recording the molar ellipticity ( $[\theta]$ ) at  $\lambda = 225$  nm, while the temperature was continuously increased in the range 10–80 °C at a rate of 0.2 °C/min. For samples exhibiting sigmoidal melting curves, the reflection point in the transition region (first derivative) is defined as the melting temperature ( $T_m$ ). Peptides and peptide-amphiphiles were dissolved in  $\text{H}_2\text{O}$  at a concentration of  $\sim 0.5$  mM at 25 °C at least 24 h prior to experiments.

**NMR Spectroscopy.** NMR spectra were acquired on a 600-MHz Varian INOVA spectrometer. Freeze-dried samples for NMR spec-

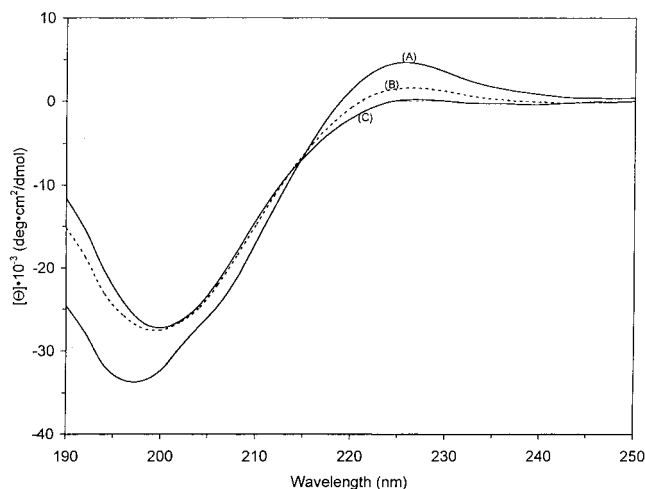


**Figure 1.** Circular dichroism spectra of the collagen-model peptide-amphiphile (A)  $\text{C}_6$ -(Gly-Pro-Hyp)<sub>4</sub>-[IV-H1]-(Gly-Pro-Hyp)<sub>4</sub> and the collagen-model peptides (B) (Gly-Pro-Hyp)<sub>4</sub>-[IV-H1]-(Gly-Pro-Hyp)<sub>4</sub> and (C) [IV-H1]-(Gly-Pro-Hyp)<sub>4</sub>. Positive values of ellipticity in the range  $\lambda = 215$ –245 nm are attributed to an ordered, polyPro II-like structure.<sup>27</sup> Among the investigated biomolecules, (Gly-Pro-Hyp)<sub>4</sub>-[IV-H1]-(Gly-Pro-Hyp)<sub>4</sub> and  $\text{C}_6$ -(Gly-Pro-Hyp)<sub>4</sub>-[IV-H1]-(Gly-Pro-Hyp)<sub>4</sub> show this structure distinctly. Peptide and peptide-amphiphile concentrations were 0.5 mM in  $\text{H}_2\text{O}$ .

troscopy were dissolved in  $\text{D}_2\text{O}$  at peptide and peptide-amphiphile concentrations of 3–5 mM at least 48 h prior to experiments. Self-diffusion coefficients ( $D$ ) were measured by pulsed-field gradient (PFG) NMR as described by Gibbs and Johnson.<sup>26</sup> Experiments were performed using a PFG duration ( $\delta$ ) of 6 ms, a time ( $\Delta$ ) of 52.4 ms between PFG pulses, and gradient strengths ( $G$ ) of 4.12, 8.24, 12.36, 16.48, 20.60, 24.72, 28.84, and 32.96 G/cm. Since samples were dissolved in  $\text{D}_2\text{O}$ , water suppression was not required.

## Results

Our ultimate goal is to design simple self-assembly systems that allow for the formation of thermally stable protein-like molecular architecture. Prior studies demonstrated that dialkyl  $\text{C}_{12}$ ,  $\text{C}_{14}$ ,  $\text{C}_{16}$ , and  $\text{C}_{18}$  tails could be used to enhance the thermal stability of triple-helical head groups.<sup>9</sup> To further investigate the effect of lipidation on stabilizing triple-helical structure, we coupled hexanoic acid to peptides containing a collagen-derived sequence ([IV-H1]) to see if a shorter single-chain lipid tail stabilizes the peptide head group structure in fashion similar to that of longer dialkyl lipid tails. We initially examined the structures of [IV-H1]-(Gly-Pro-Hyp)<sub>4</sub>, (Gly-Pro-Hyp)<sub>4</sub>-[IV-H1]-(Gly-Pro-Hyp)<sub>4</sub>, and  $\text{C}_6$ -(Gly-Pro-Hyp)<sub>4</sub>-[IV-H1]-(Gly-Pro-Hyp)<sub>4</sub> using CD spectroscopy.

Collagens in triple-helical conformation exhibit a CD spectrum similar to that of polyPro II helix, with positive ellipticity from  $\lambda = 215$ –240 nm and a minimum negative ellipticity from  $\lambda = 190$ –200 nm.<sup>27</sup> At 25 °C, both (Gly-Pro-Hyp)<sub>4</sub>-[IV-H1]-(Gly-Pro-Hyp)<sub>4</sub> and  $\text{C}_6$ -(Gly-Pro-Hyp)<sub>4</sub>-[IV-H1]-(Gly-Pro-Hyp)<sub>4</sub> exhibit CD spectra typical of triple-helical conformation (Figure 1). The amount of triple-helical conformation of  $\text{C}_6$ -(Gly-Pro-Hyp)<sub>4</sub>-[IV-H1]-(Gly-Pro-Hyp)<sub>4</sub>, as measured by molar ellipticity at  $\lambda = 225$  nm, is much higher than that of (Gly-Pro-Hyp)<sub>4</sub>-[IV-H1]-(Gly-Pro-Hyp)<sub>4</sub>. The Rpn value (the ratio of the CD maximum positive ellipticity over the minimum negative ellipticity) for the peptide-amphiphile is 0.144. [IV-H1]-(Gly-Pro-Hyp)<sub>4</sub> does not show a triple-helical CD spectrum at this

(22) (a) Fields, C. G.; Lloyd, D. H.; Macdonald, R. L.; Otteson, K. M.; Noble, R. L. *Pept. Res.* **1991**, *4*, 95–101. (b) Lauer, J. L.; Fields, C. G.; Fields, G. B. *Lett. Pept. Sci.* **1995**, *1*, 197–205.

(23) Fields, C. G.; VanDrissie, V. L.; Fields, G. B. *Pept. Res.* **1993**, *6*, 39–47.

(24) (a) Barany, G.; Merrifield, R. B. In *The Peptides*; Gross, E., Meienhofer, J., Eds.; Academic Press: New York, 1979; Vol. 2; pp 1–284. (b) Fields, G. B.; Noble, R. L. *Int. J. Pept. Protein Res.* **1990**, *35*, 161–214.

(25) (a) King, D. S.; Fields, C. G.; Fields, G. B. *Int. J. Pept. Protein Res.* **1990**, *36*, 255–266. (b) Fields, C. G.; Fields, G. B. *Tetrahedron Lett.* **1993**, *34*, 6661–6664.

(26) Gibbs, S. J.; Johnson, C. S., Jr. *J. Magn. Reson.* **1991**, *93*, 395–402.

(27) Heidemann, E.; Roth, W. *Adv. Polym. Sci.* **1982**, *43*, 143–203.



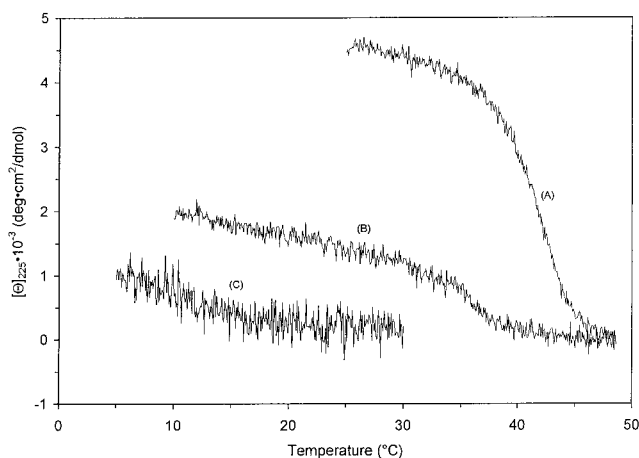


**Figure 2.** Temperature dependence of molar ellipticity at  $\lambda = 225$  nm for the collagen-model peptide-amphiphile (A)  $C_6$ -(Gly-Pro-Hyp) $_4$ -[IV-H1]-(Gly-Pro-Hyp) $_4$  and the collagen-model peptides (B) (Gly-Pro-Hyp) $_4$ -[IV-H1]-(Gly-Pro-Hyp) $_4$  and (C) [IV-H1]-(Gly-Pro-Hyp) $_4$ . Among the biomolecules, (Gly-Pro-Hyp) $_4$ -[IV-H1]-(Gly-Pro-Hyp) $_4$  and  $C_6$ -(Gly-Pro-Hyp) $_4$ -[IV-H1]-(Gly-Pro-Hyp) $_4$  display thermal denaturation curves typical for collagen-like triple helices, with  $T_m$  values of 35.6 and 42.2 °C, respectively.

temperature (Figure 1). The thermal transitions of these three peptides were monitored by measuring molar ellipticity at  $\lambda = 225$  nm as a function of increasing temperature (Figure 2). Both  $C_6$ -(Gly-Pro-Hyp) $_4$ -[IV-H1]-(Gly-Pro-Hyp) $_4$  (Figure 2A) and (Gly-Pro-Hyp) $_4$ -[IV-H1]-(Gly-Pro-Hyp) $_4$  (Figure 2B) show sigmoidal melting curves indicating a cooperative transition, which is typical of triple-helical conformation.<sup>4,8,27,28</sup> In contrast, [IV-H1]-(Gly-Pro-Hyp) $_4$  does not show this sharp transition (Figure 2C). The first derivative of the melting curves gave melting temperature ( $T_m$ ) values of 35.6 °C for (Gly-Pro-Hyp) $_4$ -[IV-H1]-(Gly-Pro-Hyp) $_4$  and 42.2 °C for  $C_6$ -(Gly-Pro-Hyp) $_4$ -[IV-H1]-(Gly-Pro-Hyp) $_4$ .

$^1\text{H}$  NMR spectroscopy was utilized to further characterize peptide and peptide-amphiphile structure. Although the CD spectra of (Gly-Pro-Hyp) $_4$ -[IV-H1]-(Gly-Pro-Hyp) $_4$  and  $C_6$ -(Gly-Pro-Hyp) $_4$ -[IV-H1]-(Gly-Pro-Hyp) $_4$  indicate triple-helix formation, these spectra represent average conformations and do not indicate which regions of the molecules are in triple-helical conformation. Our prior two-dimensional NMR studies examined the Pro and Hyp side-chain region to provide evidence that peptide-amphiphiles formed thermally stable triple helices compared with peptide alone.<sup>9</sup> However, these prior NMR experiments examined residues that were found both within and outside of the [IV-H1] sequence. While the Gly-Pro-Hyp flanking sequences are anticipated to be triple helical on the basis of prior X-ray crystallographic studies of model peptides flanked by (Gly-Pro-Hyp) $_n$ ,<sup>29</sup> the interior [IV-H1] sequence does not form a triple helix on its own.<sup>9,18</sup> Thus, we sought an NMR-based approach by which to study structure within the [IV-H1] region. To achieve this goal, NMR experiments were performed in  $\text{D}_2\text{O}$  solution. The resonance lines from labile protons are replaced in  $\text{D}_2\text{O}$ , so that the  $^1\text{H}$  NMR spectrum will contain only the resonance lines of the carbon-bound protons.<sup>30</sup> In the

case of Trp residues, resonances in the 7.0–8.0 ppm region will result from the protons attached to the 2, 4, 5, 6, and 7 positions of the side-chain indole ring.<sup>30</sup> Thus, spectra of the investigated peptides and peptide-amphiphiles in the 7.0–8.0 ppm region will result from a unique Trp residue found within the [IV-H1] sequence. To create a reference spectrum, [IV-H1]-(Gly-Pro-Hyp) $_4$  was examined. Since the Trp residue within [IV-H1]-(Gly-Pro-Hyp) $_4$  has neighboring amino acids similar to those of the Trp within (Gly-Pro-Hyp) $_4$ -[IV-H1]-(Gly-Pro-Hyp) $_4$ , the former peptide provides a reference state for the Trp residue in non-triple-helical conformation. At 25 °C, the  $^1\text{H}$  NMR spectrum showed prominent resonances at  $\sim 7.70$ , 7.68, 7.51, 7.50, 7.30, 7.26, and 7.18 ppm (Figure 3, bottom right panel). The spectrum of (Gly-Pro-Hyp) $_4$ -[IV-H1]-(Gly-Pro-Hyp) $_4$  at 40 °C (Figure 3, center left panel) is very similar to that of [IV-H1]-(Gly-Pro-Hyp) $_4$  at 25 °C. In both cases, the CD spectra (Figure 2) indicate a non-triple-helical conformation. However, the  $^1\text{H}$  NMR spectrum of (Gly-Pro-Hyp) $_4$ -[IV-H1]-(Gly-Pro-Hyp) $_4$  at 10 °C (Figure 3, upper left panel) is substantially different than that at 40 °C. In particular, there are prominent signals in the 7.71–7.78 and 7.33–7.40 ppm regions. These resonances are not due to a simple change in temperature, as the 10 °C spectrum of [IV-H1]-(Gly-Pro-Hyp) $_4$  does not contain such signals (data not shown). Since the CD data indicate that (Gly-Pro-Hyp) $_4$ -[IV-H1]-(Gly-Pro-Hyp) $_4$  is triple helical at 10 °C (Figure 2), the additional resonances in the 7.71–7.78 and 7.33–7.40 ppm regions appear to be derived from the Trp side chain in a triple-helical conformation. Increasing the temperature to 25 °C, which results in a decrease in triple helicity of (Gly-Pro-Hyp) $_4$ -[IV-H1]-(Gly-Pro-Hyp) $_4$  (Figure 2), causes a decrease in the intensities of the 7.71–7.78 and 7.33–7.40 ppm signals (Figure 3, top right panel). The  $^1\text{H}$  NMR spectrum peaks that decrease with increasing temperature may thus represent Trp within a triple-helical conformation. Some signals from (Gly-Pro-Hyp) $_4$ -[IV-H1]-(Gly-Pro-Hyp) $_4$  decrease in intensity at 40 °C but do not disappear (i.e., 7.30 and 7.57 ppm), suggesting that there is an overlap of resonance lines in triple-helical and monomeric conformations.

The  $^1\text{H}$  NMR spectra of  $C_6$ -(Gly-Pro-Hyp) $_4$ -[IV-H1]-(Gly-Pro-Hyp) $_4$  at 10 °C and 25 °C (Figure 3, center right and bottom left panels) exhibit resonance lines at chemical shifts similar to those of (Gly-Pro-Hyp) $_4$ -[IV-H1]-(Gly-Pro-Hyp) $_4$  at 10 °C (Figure 3, upper left panel). Comparing the peptide-amphiphile to (Gly-Pro-Hyp) $_4$ -[IV-H1]-(Gly-Pro-Hyp) $_4$  at the same temperatures (either 10 °C or 25 °C) indicates that the peaks corresponding to triple-helical conformation (7.71–7.78 and 7.33–7.40 ppm) are much stronger in the former compound. The peaks at 7.64–7.71 ppm, which correspond to monomeric conformation, are very weak in the spectrum of  $C_6$ -(Gly-Pro-Hyp) $_4$ -[IV-H1]-(Gly-Pro-Hyp) $_4$  at 10 °C. This result suggests that at 10 °C  $C_6$ -(Gly-Pro-Hyp) $_4$ -[IV-H1]-(Gly-Pro-Hyp) $_4$  is primarily triple helical. The thermal transitions evaluated from the NMR spectra and the CD melting curves are in agreement for both the peptides and peptide-amphiphile.

The CD and  $^1\text{H}$  NMR experiments have indicated that some NMR spectral signals arising from the side chain of Trp are associated with triple-helical conformational changes. If this is the case, than self-diffusion coefficients calculated from “triple-helical” peaks are expected to be smaller than self-diffusion coefficients calculated from “monomeric” peaks.<sup>31</sup> The self-diffusion coefficient ( $D$ ) was subsequently measured using

(28) (a) Brodsky, B.; Li, M.; Long, C. G.; Apigo, J.; Baum, J. *Biopolymers* **1992**, *32*, 447–451. (b) Anachi, R. B.; Siegel, D. L.; Baum, J.; Brodsky, B. *FEBS Lett.* **1995**, *368*, 551–555. (c) Yang, W.; Battineni, M. L.; Brodsky, B. *Biochemistry* **1997**, *36*, 6930–6935.

(29) (a) Bella, J.; Eaton, M.; Brodsky, B.; Berman, H. M. *Science* **1994**, *266*, 75–81. (b) Bella, J.; Brodsky, B.; Berman, H. M. *Structure* **1995**, *3*, 893–906.

(30) Wuthrich, K. In *NMR of Proteins and Nucleic Acids*; John Wiley & Sons: New York, 1983; pp 14–18.

(31) Li, M.; Fan, P.; Brodsky, B.; Baum, J. *Biochemistry* **1993**, *32*, 7377–7387.

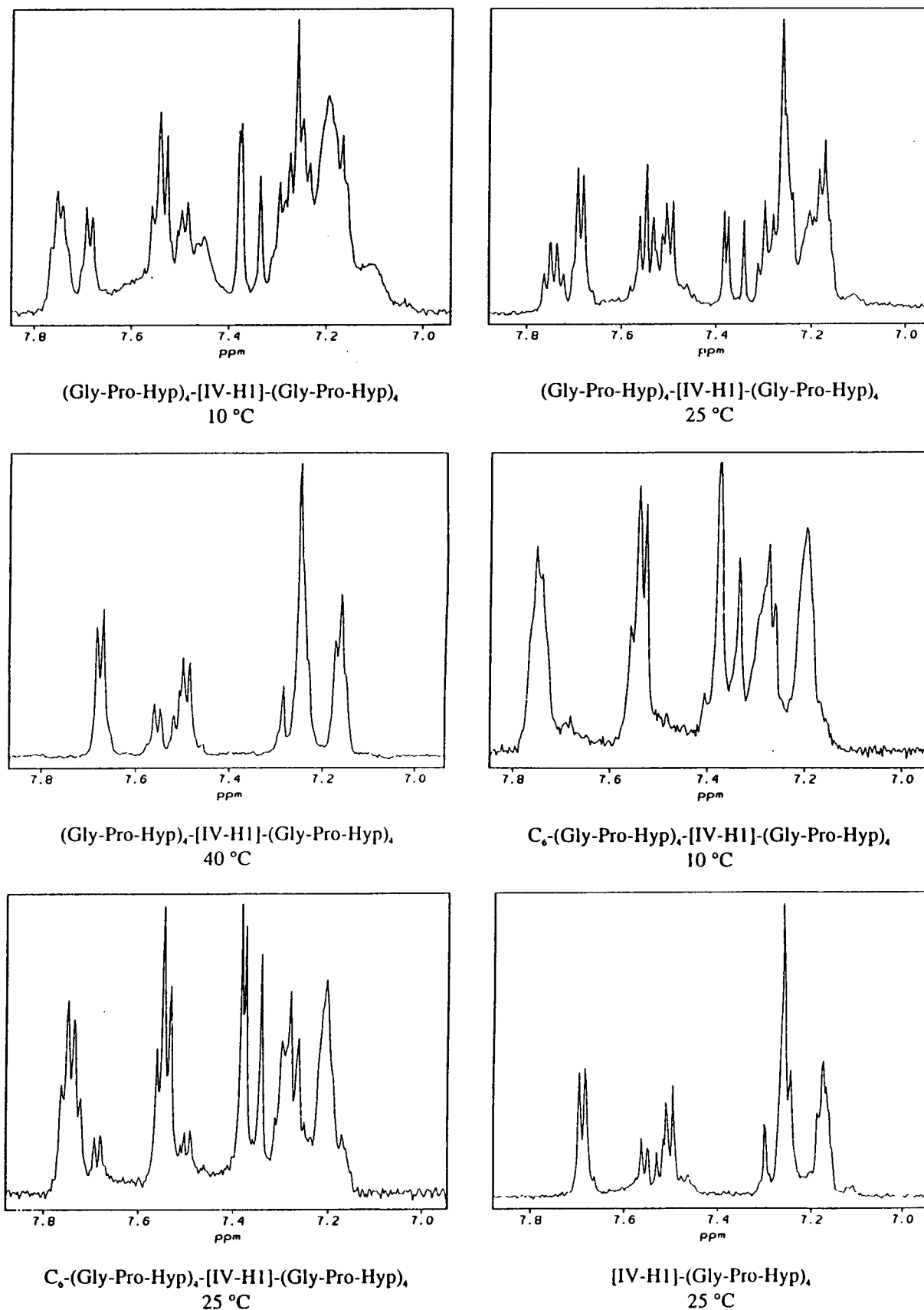


**Figure 3.** <sup>1</sup>H NMR spectra of (Gly-Pro-Hyp)<sub>4</sub>-[IV-H1]-(Gly-Pro-Hyp)<sub>4</sub> (top panels and center left panel), C<sub>6</sub>-(Gly-Pro-Hyp)<sub>4</sub>-[IV-H1]-(Gly-Pro-Hyp)<sub>4</sub> (center right and bottom left panels), and [IV-H1]-(Gly-Pro-Hyp)<sub>4</sub> (bottom right panel) in D<sub>2</sub>O at 10, 25, or 40 °C. Peptide and peptide-amphiphile concentrations were 5 mM. Resonances in the 7.0–8.0 ppm region result from the protons attached to the 2, 4, 5, 6, and 7 positions of the side-chain indole ring from a unique Trp residue found within the [IV-H1] sequence. By comparison with the CD-derived melting temperatures for the peptides and peptide-amphiphile, the peaks at 7.64–7.71 ppm correspond to monomeric conformation while those at 7.71–7.78 and 7.33–7.40 ppm correspond to triple-helical conformation.

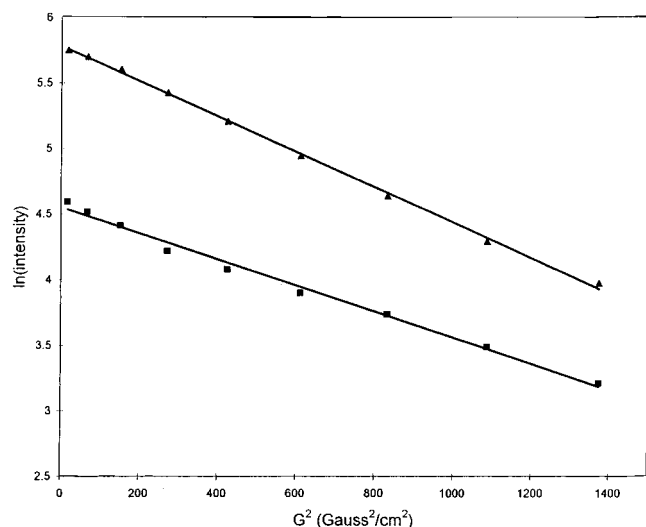


**Figure 4.** Plot of signal attenuation versus  $G^2$  for  $^1\text{H}$  NMR signals at 7.70 ppm (upper line) and 7.74 ppm (lower line) from the PFG experiment. The self-diffusion coefficients ( $D$ ) (line slope) are  $1.02 \times 10^{-6}$  and  $0.69 \times 10^{-6}$   $\text{cm}^2/\text{s}$  for the 7.70 and 7.74 ppm signals, respectively. This indicates that the species corresponding to the 7.70 ppm signal exhibits a different, higher diffusion coefficient than the species corresponding to the 7.74 ppm.

PFG NMR spectroscopy and varying the gradient strength. The results were fitted to eq 1:

$$A = A_0 \exp[-(\gamma\delta G)^2(\Delta - \delta/3)D] \quad (1)$$

where  $A$  is the NMR signal strength,  $A_0$  is the NMR signal strength in the absence of gradient,  $\gamma$  is the  $^1\text{H}$  gyromagnetic ratio,  $\delta$  is PFG duration,  $G$  is the gradient strength, and  $\Delta$  is the time between PFG pulses.  $D$  was initially measured for the peaks occurring at 7.74 ppm, potentially corresponding to triple-helical conformation, and 7.70 ppm, potentially corresponding to monomeric conformation (Figure 4). The two curves generated have different slopes, and thus different  $D$  values, indicating that they correspond to different states and are in slow exchange on the time scale of the experiment. The  $D$  values calculated at 7.74 and 7.70 ppm are  $0.69 \times 10^{-6}$  and  $1.02 \times 10^{-6}$   $\text{cm}^2/\text{s}$ , respectively. Thus,  $D$  is lower for the "triple-helical" peak compared with the "monomeric" peak.

Self-diffusion coefficients were next measured for peaks at chemical shifts occurring between 7.0 and 8.0 ppm (Figure 5).  $D$  values were found to be in one of three ranges,  $0.6\text{--}0.7 \times 10^{-6}$ ,  $0.7\text{--}0.95 \times 10^{-6}$ , or  $0.95\text{--}1.1 \times 10^{-6}$   $\text{cm}^2/\text{s}$ . Peaks corresponding to triple-helical conformation would fall into the lowest  $D$  value range, while those corresponding to nontriple-helical conformation fall into the highest  $D$  value range. The peaks that exist in both states assume intermediate values when results are fitted to eq 1. Signals in the ranges 7.76–7.70 and 7.39–7.31 ppm appear to be unique for triple-helical conformation, while those in the ranges 7.68–7.65, 7.51–7.48, and 7.26–7.24 ppm are unique for monomeric conformation.

The addition of a  $\text{C}_6$  monoalkyl tail has been found to enhance the triple-helical thermal stability of the  $(\text{Gly-Pro-Hyp})_4\text{-[IV-HI]-(Gly-Pro-Hyp)}_4$  sequence (Figure 2). Other monoalkyl tails were thus studied for their affect on triple-helical stability. Peptide-amphiphiles of the sequence  $\text{C}_n\text{-(Gly-Pro-Hyp)}_4\text{-[IV-HI]-(Gly-Pro-Hyp)}_4$ , where  $n = 6, 8, 10, 12, 14,$  or  $16$ , were all found to exhibit CD spectra typical of triple-helical conformation (data not shown). The thermal transitions for these peptide-amphiphiles were sigmoidal, indicating a cooperative

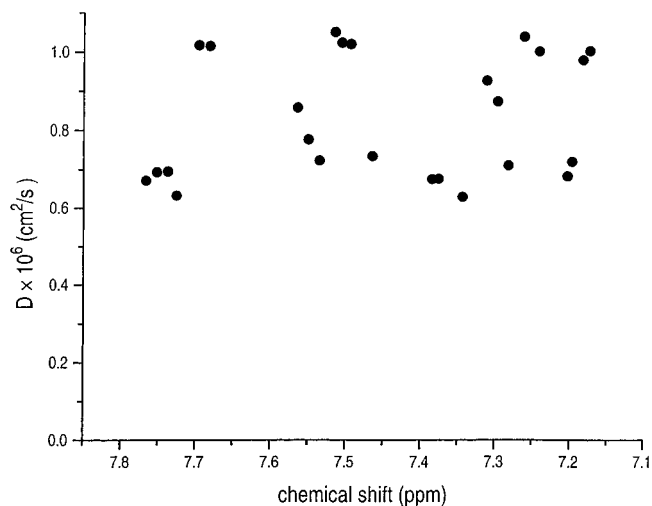


**Figure 5.** Self-diffusion coefficients ( $D$ ) of  $^1\text{H}$  NMR peaks occurring over the chemical shift range 7.1–7.8 ppm.  $D$  may be classified as either  $0.6\text{--}0.7 \times 10^{-6}$   $\text{cm}^2/\text{s}$ , which corresponds to peaks that decrease with increasing temperature,  $1.0 \times 10^{-6}$   $\text{cm}^2/\text{s}$ , which corresponds to peaks that increase with increasing temperature, or  $>0.7$  but  $<0.9 \times 10^{-6}$   $\text{cm}^2/\text{s}$ . Signals in the ranges 7.76–7.70 and 7.39–7.31 ppm appear to be unique for triple-helical conformation, while those in the ranges 7.68–7.65, 7.51–7.48, and 7.26–7.24 ppm are unique for monomeric conformation.

transition (Figure 6).  $T_m$  values were calculated from the first derivative of the melting curves.<sup>32</sup>  $T_m$  values were found to increase with monoalkyl tail chain length (Table 1).

## Discussion

A vast number of approaches have been described by which protein-like molecular architecture can be created and stabilized. We have recently examined the use of lipophilic of compounds for potentially aligning peptide strands and inducing and/or stabilizing protein-like secondary, supersecondary, and tertiary structures within these peptide sequences.<sup>9,10,21</sup> Our initial studies demonstrated that dialkyl ester compounds of carbon chain lengths 12–18 stabilize triple-helical conformation.<sup>9,10</sup> In the present study, we have examined monoalkyl chains to determine if they exert a similar stabilizing effect on protein-like structure.

The triple helix consists of three intertwined peptide chains, each chain in polyPro II-like conformation. The unique steric requirements of Pro led to two well-characterized conformations for polyPro, referred to as polyPro I and polyPro II helices. In aqueous solution and other polar solvents, polyPro II helices are favored. The CD spectrum of polyPro II helix has a positive band at  $\lambda = 226$  nm and a strong negative band at  $\lambda = 190$  nm.<sup>33</sup> Triple helices and polyPro II structures exhibit CD spectra that are similar to each other but distinct from other secondary/supersecondary structures. The confirmation of triple-helical structure requires several criteria. These criteria can be based on studies of  $(\text{Pro-Pro-Gly})_{10}$  and  $(\text{Pro-Hyp-Gly})_4\text{-Pro-Hyp-Ala-(Pro-Hyp-Gly)}_5$ , the only triple-helical peptides for which exist a complete set of X-ray crystallographic and CD and NMR spectroscopic data. The X-ray crystallographic structures of  $(\text{Pro-Pro-Gly})_{10}$ <sup>34</sup> and  $(\text{Pro-Hyp-Gly})_4\text{-Pro-Hyp-Ala-(Pro-Hyp-Gly)}_5$ <sup>29</sup> are comparable to that observed for type I collagen.<sup>35</sup>

(32) Venugopal, M. G.; Ramshaw, J. A. M.; Braswell, E.; Zhu, D.; Brodsky, B. *Biochemistry* **1994**, *33*, 7948–7956.

(33) Woody, R. W. In *The Peptides*; Udenfriend, S., Meienhofer, J., Eds.; Academic Press: New York, 1985; Vol. 7, pp 15–114.

(34) Okuyama, K.; Okuyama, K.; Arnott, S.; Takayanagi, M.; Kakudo, M. *J. Mol. Biol.* **1981**, *152*, 427–443.

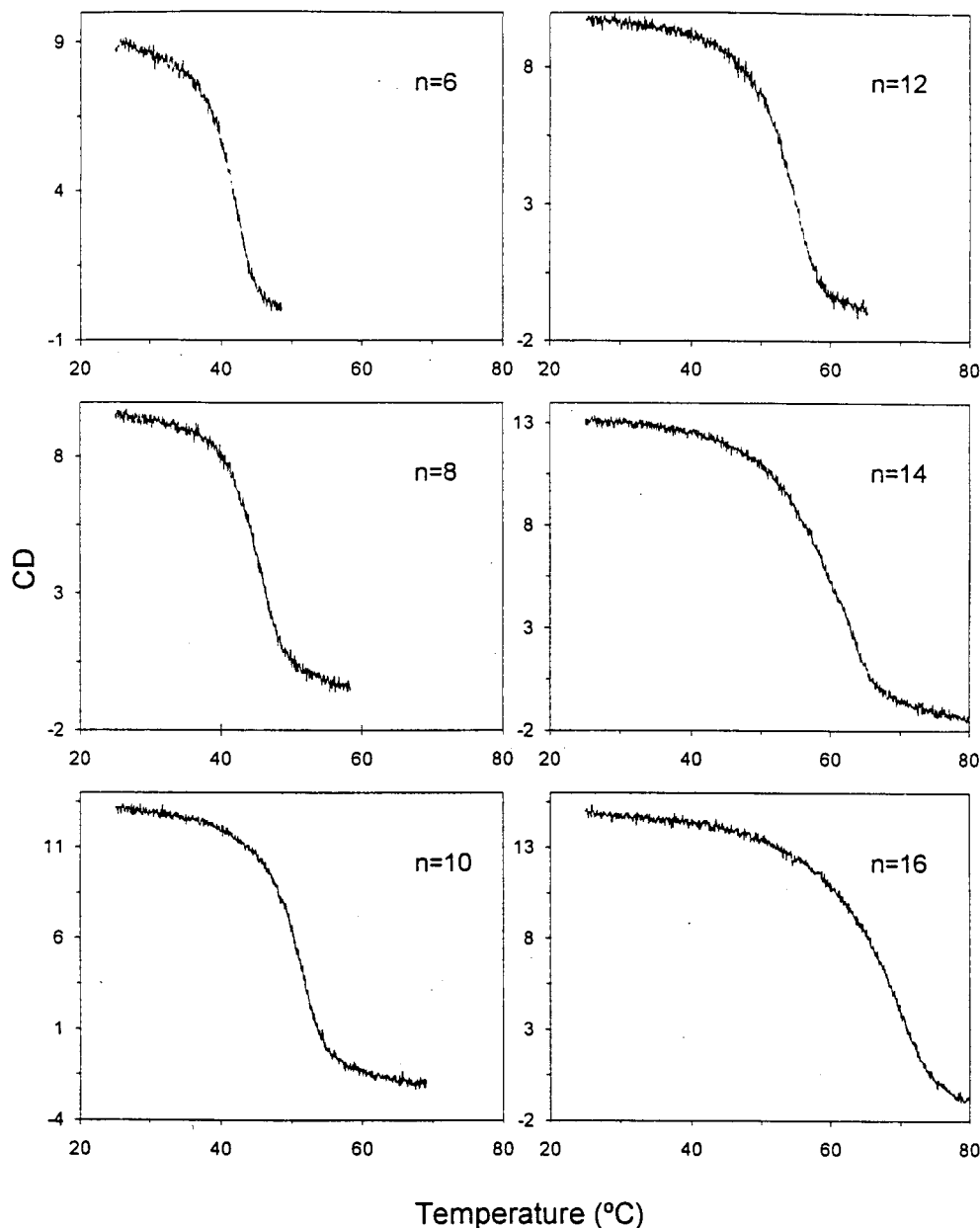


**Figure 6.** Temperature dependence of CD spectra at  $\lambda = 225$  nm for collagen-model peptide-amphiphiles. Monoalkyl tail chain ( $C_n$ ) length ranges from 6 to 16 carbon atoms. All of the peptide-amphiphiles display thermal denaturation curves typical for collagen-like triple helices. The slightly broader transitions seen for the  $C_{14}$ - and  $C_{16}$ -peptide-amphiphiles are due to transitions from aggregated triple helices to denatured species.  $T_m$  values are given in Table 1.

**Table 1.**  $T_m$  Values for Peptide and Peptide-Amphiphile Triple Helix  $\leftrightarrow$  Coil Transitions

peptide or peptide-amphiphile	$T_m$ (°C)
(Gly-Pro-Hyp) <sub>4</sub> -[IV-HI]-(Gly-Pro-Hyp) <sub>4</sub>	35.6
C <sub>6</sub> -(Gly-Pro-Hyp) <sub>4</sub> -[IV-HI]-(Gly-Pro-Hyp) <sub>4</sub>	42.2
C <sub>8</sub> -(Gly-Pro-Hyp) <sub>4</sub> -[IV-HI]-(Gly-Pro-Hyp) <sub>4</sub>	45.6
C <sub>10</sub> -(Gly-Pro-Hyp) <sub>4</sub> -[IV-HI]-(Gly-Pro-Hyp) <sub>4</sub>	51.3
C <sub>12</sub> -(Gly-Pro-Hyp) <sub>4</sub> -[IV-HI]-(Gly-Pro-Hyp) <sub>4</sub>	55.0
C <sub>14</sub> -(Gly-Pro-Hyp) <sub>4</sub> -[IV-HI]-(Gly-Pro-Hyp) <sub>4</sub>	63.1
C <sub>16</sub> -(Gly-Pro-Hyp) <sub>4</sub> -[IV-HI]-(Gly-Pro-Hyp) <sub>4</sub>	69.8
(C <sub>12</sub> ) <sub>2</sub> -(Gly-Pro-Hyp) <sub>4</sub> -[IV-HI]-(Gly-Pro-Hyp) <sub>4</sub>	71.2 <sup>51</sup>

Both peptides exhibit CD spectra similar to that of collagen, with a maximum, positive molar ellipticity at 220–224 nm and

a minimum, negative molar ellipticity at 198–200 nm.<sup>36–38</sup> Sharp sigmoidal transitions are observed as a function of temperature for (Pro-Pro-Gly)<sub>10</sub> and (Pro-Hyp-Gly)<sub>4</sub>-Pro-Hyp-Ala-(Pro-Hyp-Gly)<sub>5</sub>, with  $T_m$  values of 28 and 29.3 °C, respectively.<sup>37,38</sup> Type I collagen exhibits a sharp sigmoidal transition with increasing temperature;  $T_m$  values are on the order of 36–41 °C.<sup>39</sup> PolyPro II helices do not exhibit sigmoidal melting transitions.<sup>27</sup> Finally, one-dimensional <sup>1</sup>H NMR has shown that individual residue side chains within the two peptides are sensitive to triple-helical environment, i.e., specific signals may shift or disappear upon transition from triple-helical to

(36) Shaw, B. R.; Schurr, J. M. *Biopolymers* **1975**, *14*, 1951–1985.

(37) Engel, J.; Chen, H.-T.; Prockop, D. J.; Klump, K. *Biopolymers* **1977**, *16*, 601–622.

(38) (a) Long, C. G.; Li, M. H.; Baum, J.; Brodsky, B. *J. Mol. Biol.* **1992**, *225*, 1–4. (b) Long, C. G.; Braswell, E.; Zhu, D.; Apigo, J.; Baum, J.; Brodsky, B. *Biochemistry* **1993**, *32*, 11688–11695.

(39) Privalov, P. *Adv. Protein Chem.* **1982**, *35*, 1–104.

(35) (a) Fraser, R. D. B.; MacRae, T. P.; Suzuki, E. *J. Mol. Biol.* **1979**, *129*, 463–481. (b) Fraser, R. D. B.; MacRae, T. P.; Miller, A.; Suzuki, E. *J. Mol. Biol.* **1983**, *167*, 497–521.



monomeric species.<sup>38,40,41</sup> Melting transitions monitored by CD and <sup>1</sup>H NMR spectroscopies are virtually identical.<sup>38</sup> Although an X-ray crystallographic structure has not been obtained, (Pro-Hyp-Gly)<sub>10</sub> shows the same general CD and NMR spectroscopic behaviors as (Pro-Pro-Gly)<sub>10</sub> and (Pro-Hyp-Gly)<sub>4</sub>-Pro-Hyp-Ala-(Pro-Hyp-Gly)<sub>5</sub>, with a *T*<sub>m</sub> value of 57.5 °C.<sup>37,38,42</sup> Two-dimensional NMR has been used to characterize the triple-helical structure and dynamics of (Pro-Hyp-Gly)<sub>10</sub>.<sup>31,43</sup> (Pro-Hyp-Gly)<sub>10</sub> has been used to develop another parameter to characterize triple helicity, the Rpn value.<sup>42</sup> Rpn values greater than 0.12 are indicative of triple helicity.<sup>42</sup>

The CD spectra for (Gly-Pro-Hyp)<sub>4</sub>-[IV-H1]-(Gly-Pro-Hyp)<sub>4</sub> and C<sub>6</sub>-(Gly-Pro-Hyp)<sub>4</sub>-[IV-H1]-(Gly-Pro-Hyp)<sub>4</sub> (Figure 1) are indicative of collagen-like triple helices. An increase in triple-helical thermal stability is manifested by a shift in the wavelength of the minimum, negative ellipticity to values below 200 nm.<sup>42</sup> We see such a shift for the C<sub>6</sub>-peptide-amphiphile compared to the peptide alone (Figure 1). The Rpn value for the C<sub>6</sub>-peptide-amphiphile (0.144) suggests a triple-helical structure. The CD spectrum of the C<sub>6</sub>-peptide-amphiphile shows a small shoulder in the range of λ = 200–207 nm (Figure 1), which may be due to some slight perturbation of the overall structure. We are further examining the dynamics of the C<sub>6</sub>-peptide-amphiphile by two-dimensional NMR techniques, which will be reported elsewhere. CD monitoring of the thermal denaturation of (Gly-Pro-Hyp)<sub>4</sub>-[IV-H1]-(Gly-Pro-Hyp)<sub>4</sub> and C<sub>6</sub>-(Gly-Pro-Hyp)<sub>4</sub>-[IV-H1]-(Gly-Pro-Hyp)<sub>4</sub> indicates that both contain triple-helical structures, while [IV-H1]-(Gly-Pro-Hyp)<sub>4</sub> is assumed to be non-triple-helical on the basis of the lack of a sigmoidal melting curve (Figure 2).

We have found that lack of a (Gly-Pro-Hyp)<sub>4</sub> region at the peptide N-terminus [i.e., [IV-H1]-(Gly-Pro-Hyp)<sub>4</sub>] or increasing temperature [i.e., (Gly-Pro-Hyp)<sub>4</sub>-[IV-H1]-(Gly-Pro-Hyp)<sub>4</sub> at 40 °C] are two different mechanisms for eliminating triple-helical structure. Comparison of these two mechanisms by NMR indicated that the resulting spectra are similar (Figure 3, center left and bottom right). By analyzing the region of the NMR spectrum encompassed by Trp side-chain protons, we discovered that the indole protons of Trp residues appear to be sensitive to triple-helical conformation. Other researchers have found similar conformational sensitivities among amino acid side-chain protons. For example, Long et al.<sup>38</sup> and Feng et al.<sup>42</sup> demonstrated that the C<sub>δ</sub>H of Pro at 3.2 ppm is sensitive to triple-helical conformation and thus triple-helicity could be monitored by one-dimensional <sup>1</sup>H NMR. Melacini et al.<sup>44</sup> determined that the C<sub>β</sub>H<sub>3</sub> and C<sub>β</sub>H<sub>1,h</sub> of Nleu are sensitive to triple-helical conformation. On the basis of our one-dimensional NMR spectra, the Trp residue within the [IV-H1] region of (Gly-Pro-Hyp)<sub>4</sub>-[IV-H1]-(Gly-Pro-Hyp)<sub>4</sub> and C<sub>6</sub>-(Gly-Pro-Hyp)<sub>4</sub>-[IV-H1]-(Gly-Pro-Hyp)<sub>4</sub> is in a triple-helical environment at low temperature.

Self-diffusion is the translational motion reflecting the random motions of a molecule in the absence of a concentration gradient and is commonly used to determine the oligomeric state of a biomolecular system. Diffusion coefficients depend on the size

of the biomolecules, with the triple helix anticipated to have a smaller diffusion coefficient than the non-triple-helix (monomer). Thus, diffusion coefficients could provide additional evidence for the distinction between triple-helical and monomeric species. The self-diffusion coefficient values were 1.02 × 10<sup>-6</sup> cm<sup>2</sup>/s for the presumed non-triple-helical species and 0.69 × 10<sup>-6</sup> cm<sup>2</sup>/s for the presumed triple-helical species. The value for the non-triple-helical species is lower than that for IV-H1 itself,<sup>45</sup> which is anticipated on the basis of the additional monoalkyl C<sub>6</sub> group and the (Gly-Pro-Hyp)<sub>4</sub> repeats. The value for the triple-helical species is in the range 65–70 kDa for globular proteins,<sup>45</sup> which is also anticipated on the basis of the rodlike structure and anisotropic motion of a triple helix.<sup>31,46</sup> If one considers type I collagen, the prolate ellipsoid shape of the protein results in a diffusion coefficient (*D*<sup>o</sup>) value of 0.69 × 10<sup>-7</sup> cm<sup>2</sup>/s, ~5.5 times lower than a spherical (globular) protein of similar mass (345 kDa).<sup>47</sup> Thus, the self-diffusion coefficients measured here by PFG NMR, along with the sharp signals observed in the one-dimensional <sup>1</sup>H NMR spectra, support the presence and identity of a nonaggregated triple-helical species at lower temperature and a monomeric species at higher temperature.

The NMR and CD spectroscopic studies presented here provide strong evidence that (1) the C<sub>6</sub>-peptide-amphiphile is in a predominantly triple-helical conformation at temperatures below 30 °C, (2) the [IV-H1] region within the peptide-amphiphile is in a triple-helical environment, and (3) there exist two peptide-amphiphile states, one at low temperature and one at high temperature, of different diffusion coefficients. The evidence for triple helicity is based upon (1) CD spectra characteristic of triple helices, (2) Rpn values in the range of triple-helical values, (3) sigmoidal melting curves for the transition from the triple-helix to monomeric state, (4) one-dimensional <sup>1</sup>H NMR spectra correlating shifts in Trp proton signals with melting transitions observed by CD spectroscopy, and (5) PFG NMR determination of self-diffusion coefficients for two distinct species correlated to the melting transitions observed by CD spectroscopy.

An increase in peptide-amphiphile alkyl chain length results in an increase of triple-helical head-group melting temperature. As shown by Feng et al., simply acetylating the N-terminus of a triple-helical sequence such as (Gly-Pro-Hyp)<sub>n</sub> increases the *T*<sub>m</sub> value.<sup>42</sup> The continued increase in thermal stability suggests that simply “capping” the triple helix is not the only mechanism at work; hydrophobic interactions between the alkyl chains can act to further stabilize the triple helix. As we discussed previously,<sup>9</sup> the role of the lipophilic tail appears to be to shift the equilibrium between folded and unfolded states, resulting in enhanced thermal stabilities. It is possible that additional inductive effects<sup>48</sup> contribute to enhanced thermal stability of the triple-helical head group. The sharper melting transitions observed in the present study (Figure 6) compared to broader melting transitions for dialkyl peptide-amphiphiles<sup>9</sup> is indicative of the aggregation state of the triple helices. For example, monoalkyl peptide-amphiphiles exist primarily as monomeric triple helices, while the dialkyl peptide-amphiphiles appear to exist as aggregated triple helices. Comparison of one-dimensional NMR spectra show that line broadening occurs in

(45) Daragan, V. A.; Ilyina, E.; Mayo, K. H. *Biopolymers* **1993**, *33*, 521–533.

(46) Torchia, D. A.; Lyerla, J. R., Jr.; Quattrone, A. J. *Biochemistry* **1975**, *14*, 887–900.

(47) Tanford, C. In *Physical Chemistry of Macromolecules*; John Wiley & Sons: New York, 1961; p 358.

(48) Holmgren, S. K.; Taylor, K. M.; Bretscher, L. E.; Raines, R. T. *Nature* **1998**, *392*, 666–667.

(40) Kobayashi, Y.; Kyogoku, Y. *J. Mol. Biol.* **1973**, *81*, 337–347.

(41) Bhatnagar, R.; Pattabiraman, N.; Sorensen, K. R.; Langridge, R.; MacElroy, R. D.; Renugopalakrishnan, V. *J. Biomol. Struct. Dyn.* **1988**, *6*, 223–233.

(42) Feng, Y.; Melacini, G.; Taulane, J. P.; Goodman, M. *J. Am. Chem. Soc.* **1996**, *118*, 10351–10358.

(43) Fan, P.; Li, M.-H.; Brodsky, B.; Baum, J. *Biochemistry* **1993**, *32*, 13299–13309.

(44) (a) Melacini, G.; Feng, Y.; Goodman, M. *J. Am. Chem. Soc.* **1996**, *118*, 10725–10732. (b) Melacini, G.; Feng, Y.; Goodman, M. *Biochemistry* **1997**, *36*, 8725–8732.



dialkyl peptide-amphiphiles<sup>21</sup> compared with monoalkyl peptide-amphiphiles (Figure 3). The longer chain monoalkyl peptide-amphiphiles (C<sub>14</sub> and C<sub>16</sub>) appear to aggregate, resulting in broader melting curves (Figure 6). An exact thermodynamic analysis of the melting transition and effects of alkyl tails is difficult, as thermodynamic parameters themselves increase as a function of increasing temperature for transfer of hydrocarbons/nonpolar molecules from liquid phase to water.<sup>49</sup> However, at a given temperature (i.e., 298 K), transfer from organic solvents to water for alkanes of increasing length is reflected by increasing enthalpic and slightly decreasing entropic values.<sup>50</sup>

The triple helix is exceptionally stable when formed in the presence of the lipid modification. The effects of lipid tails on collagenous head groups are significant, despite the small size of the former compounds. For example, the difference in the denaturation temperatures between the structured (Gly-Pro-Hyp)<sub>4</sub>-[IV-H1]-(Gly-Pro-Hyp)<sub>4</sub> peptide ( $T_m = 35.6$  °C)<sup>9</sup> and the corresponding C<sub>16</sub> peptide-amphiphile is 34.2 °C. The enhanced stability is not quite equal to that of a dialkyl chain tail, however. For example, the C<sub>12</sub> monoalkyl peptide-amphiphile has a  $T_m = 55.0$  °C, while the C<sub>12</sub> dialkyl peptide-amphiphile has a  $T_m = 71.2$  °C.<sup>9,51</sup> However, although monoalkyl and dialkyl chains are quite different in their structures, their *overall* effects on the structure and stability of peptide head groups are similar. This may be due to the flexibility of the alkyl chain and/or the hydrophobic interaction that drives the lipid tails together. Since the lipid tails do not interfere with the folding of the triple-helical peptide head group, lipid tails may be ideal building blocks for protein-like molecular architecture.

There is now considerable evidence to suggest that peptide-lipids can oligomerize and form a variety of stable structures. We have demonstrated that dialkyl C<sub>12</sub>-C<sub>18</sub> or monoalkyl C<sub>6</sub>-C<sub>16</sub> chains can be used to stabilize triple-helical structure. Additional recent work from our laboratory has indicated that

(49) Privalov, P. L.; Gill, S. J. *Adv. Protein Chem.* **1988**, *39*, 191-233.

(50) Tanford, C. In *The Hydrophobic Effect*, 2nd ed.; John Wiley & Sons: New York, 1980; p 24.

(51) Yu, Y.-C. Synthesis and Characterization of Collagenous Peptide-Amphiphiles. Ph.D. Dissertation, University of Minnesota: Minneapolis, MN, 1997; pp 59-60.

$\alpha$ -helical structures are stabilized by alkyl chains.<sup>19</sup> The stability of peptide-lipid structures has been observed in several other laboratories. For example, when the peptide acetyl-Lys-Gly-Arg-Gly-Asp-Gly amide is attached to dodecyl phosphocholine via the *N*<sup>ε</sup>-amino group of Lys, 2D <sup>1</sup>H NMR indicated that the peptide-amphiphile forms a turn conformation (type II or I') while the peptide itself mixed with the phospholipid does not.<sup>52</sup> An FTIR reflection absorption spectroscopic study of *N*-octadecanoyl (Gly)<sub>*n*</sub> ethyl ester monolayers and Langmuir-Blodgett films, where *n* = 1-5, demonstrated that the peptide-amphiphiles could form polyGly II helices while the oligoGly peptides themselves could not.<sup>53</sup> CD studies of (sarcosine)<sub>3</sub> or (Pro)<sub>4</sub> coupled to dialkyl amide chains indicated a regular arrangement of amide and/or imide groups.<sup>54</sup>

The peptide-amphiphile system appears to be versatile for creating and stabilizing desired molecular architectures. Such architectures could be used to further study protein folding,<sup>55</sup> to produce novel bioactive proteins,<sup>19</sup> and to coat biomaterial surfaces to enhance biocompatibility.<sup>10,19</sup> The interaction of peptide-amphiphiles with cell surface receptors may mimic fusion of viral envelopes with cellular membranes,<sup>56</sup> and thus peptide-amphiphiles could also be utilized as drug delivery vehicles.

**Acknowledgment.** This research is supported from the Center for Interfacial Engineering (an NSF ERC), the Earl E. Bakken Chair for Biomedical Engineering, and NIH Grants CA77402, HL62427, and AR01929.

JA981654Z

(52) Macquaire, F.; Baleux, F.; Giaccobi, E.; Huynh-Dinh, T.; Neumann, J.-M.; Sanson, A. *Biochemistry* **1992**, *31*, 2576-2582.

(53) Cha, X.; Ariga, K.; Kunitake, T. *Bull. Chem. Soc. Jpn.* **1996**, *69*, 163-168.

(54) Shimizu, T.; Mori, M.; Minamikawa, H.; Hato, M. *Chem. Lett.* **1989**, 1341-1344.

(55) Bulleid, N. J.; Dalley, J. A.; Lees, J. F. *EMBO J.* **1997**, *16*, 6694-6701.

(56) (a) Ohnishi, S.-I. *Curr. Top. Membr. Transp.* **1988**, *32*, 257-295.  
(b) Bagai, S.; Sarkar, D. P. *Biochim. Biophys. Acta* **1993**, *1152*, 15-25.